

Coupled stratigraphic and U-Pb zircon age constraints on the late Paleozoic icehouse-to-greenhouse turnover in south-central Gondwana

Neil Patrick Griffis^{1,2*}, Isabel Patricia Montañez¹, Roland Mundil², Jon Richey¹, John Isbell³, Nick Fedorchuk³, Bastien Linol⁴, Roberto Iannuzzi⁵, Fernando Vesely⁶, Thammy Mottin⁶, Eduardo da Rosa⁶, Brenhin Keller² and Qing-Zhu Yin¹

¹Department of Earth and Planetary Sciences, University of California, Davis, California 95616, USA

²Berkeley Geochronology Center, Berkeley, California 94709, USA

³Department of Geosciences, University of Wisconsin, Milwaukee, Wisconsin 53211, USA

⁴Department of Geosciences, Nelson Mandela University, Port Elizabeth 6019, South Africa

⁵Departamento de Paleontologia e Estratigrafia, Universidade Federal Rio Grande do Sul, Porto Alegre, RS, 90040-060, Brazil

⁶Departamento de Geologia, Universidade Federal do Paraná, Curitiba, PR, 80060-000, Brazil

ABSTRACT

The demise of the Late Paleozoic Ice Age has been hypothesized as diachronous, occurring first in western South America and progressing eastward across Africa and culminating in Australia over an ~60 m.y. period, suggesting tectonic forcing mechanisms that operate on time scales of 10^6 yr or longer. We test this diachronous deglaciation hypothesis for southwestern and south-central Gondwana with new single crystal U-Pb zircon chemical abrasion thermal ionizing mass spectrometry (CA-TIMS) ages from volcanoclastic deposits in the Paraná (Brazil) and Karoo (South Africa) Basins that span the terminal deglaciation through the early postglacial period. Intrabasinal stratigraphic correlations permitted by the new high-resolution radioisotope ages indicate that deglaciation across the S to SE Paraná Basin was synchronous, with glaciation constrained to the Carboniferous. Cross-basin correlation reveals two additional glacial-deglacial cycles in the Karoo Basin after the terminal deglaciation in the Paraná Basin. South African glaciations were penecontemporaneous (within U-Pb age uncertainties) with third-order sequence boundaries (i.e., inferred base-level falls) in the Paraná Basin. Synchronicity between early Permian glacial-deglacial events in southwestern to south-central Gondwana and $p\text{CO}_2$ fluctuations suggest a primary CO_2 control on ice thresholds. The occurrence of renewed glaciation in the Karoo Basin, after terminal deglaciation in the Paraná Basin, reflects the secondary influences of regional paleogeography, topography, and moisture sources.

INTRODUCTION

The Late Paleozoic Ice Age (LPIA), spanning 340–280 Ma, has produced the only known archive of a permanent icehouse-to-greenhouse turnover on a planet populated by complex terrestrial ecosystems and metazoan life (Gastaldo et al., 1996). The spatial and temporal distribution of continental ice throughout southern Gondwana during the LPIA and its ultimate demise have been attributed in large part to the long-term (10^7 to 10^8 yr) drift of southern Gondwana away from the South Pole during the Carboniferous–Permian (Crowell, 1983; Li-

marino et al., 2014) as well as tectonic controls (Visser, 1997). Alternatively, CO_2 forcing has been hypothesized as the primary driver of the repeated, discrete glaciations and intervening periods of diminished ice, and the ultimate turnover to permanent greenhouse conditions (Montañez et al., 2007, 2016). Although these two proposed forcing mechanisms (tectonic versus climate) for the late Paleozoic glaciation history are interlinked through the influence of large-scale tectonics on CO_2 sources (i.e., volcanism) and sinks and through atmospheric and ocean circulation (McKenzie et al., 2016; Montañez et al., 2016), the two mechanisms differ in their temporal scales of influence on ice distribution

and dynamics. Tectonic controls would have operated on 10^6 to 10^7 yr time scales and resulted in a diachronous glacial record across high-latitude Gondwana (Isbell et al., 2012; Limarino et al., 2014). Late Paleozoic climate simulations, however, do not support a tectonic drift model for ice initiation thresholds (Lowry et al., 2014). Conversely, a CO_2 driver would have operated on shorter time scales, analogous with the Cenozoic glaciation history of Antarctica (Miller et al., 2005). Notably, CO_2 -forced deglaciation (and associated base-level changes) would be expected to have been rapid (10^3 to 10^5 yr) and thus broadly synchronous across multiple basins.

The precision and distribution of existing U-Pb age constraints for ice-proximal deposits of southern Gondwana precludes evaluation of the relative influence of hypothesized glaciation-deglaciation drivers and their role in the ultimate turnover to a permanent greenhouse in the middle Permian. Here we present a temporally refined record of glaciation in southwestern to south-central Gondwana across the latest Carboniferous and early Permian, built using high-precision, single-crystal zircon U-Pb chemical abrasion thermal ionizing mass spectrometry (CA-TIMS) dating of volcanoclastic deposits located within the earliest postglacial sediments of the Paraná Basin, Brazil, and two glacial-deglacial cycles (deglaciation sequences DS III and DS IV) in the Karoo Basin, South Africa (Visser, 1997). The new chronostratigraphic framework is used to evaluate the synchronicity of ice loss across this region and to evaluate the

*E-mail: npgriffis@ucdavis.edu

base-level response in the Paraná Basin to the higher-latitude ice record (Karoo Basin) during the early Permian.

GEOLOGIC SETTING, STRATIGRAPHY, AND EXISTING U-Pb GEOCHRONOLOGY

The Paraná and Karoo Basins span a collective area of 2.3×10^6 km² and were the largest depocenters of LPIA sediment accumulation in southwestern to south-central Gondwana (Fig. 1). The Paraná Basin, located between 40°S and 55°S during the earliest Permian (Franco et al., 2012; Domeier and Torsvik, 2014), records an extensive record of paleo-glaciation within the Itararé Group (Rocha-Campos et al., 2008). Record of the demise of glaciation in the

Paraná Basin occurs within the upper Taciba Formation (Itararé Group), composed of diamictite and dropstone-poor mudstones (Fig. 1; Vesely and Assine, 2004). The terrestrial and marginal marine facies assemblage of the Guatá Group, which include the Rio Bonito and Palermo Formations, overlay the Itararé Group and attain a maximum thickness of 300 m (Fig. 1; Rocha-Campos et al., 2008; Holz et al., 2010). In southeastern Paraná Basin, the Rio Bonito Formation is further divided into the Triunfo, Paraguaçu, and Siderópolis Members (Schneider et al., 1974), which are not formally recognized in the southern Paraná Basin. However, sequence boundaries SB-2 and SB-3, which bracket these members, are correlated between regions (Fig. 1; Holz et al., 2006; Iannuzzi et al., 2010).

Two third-order depositional sequences, previously suggested to have been controlled by regional tectonic forcing (Holz et al., 2006), occur in the latest Carboniferous through early Permian sedimentary record of the Paraná Basin. The first sequence boundary (SB-2 of Holz et al. [2006]) separates deeper-water glacially influenced diamictites and organic mudstones of the Taciba Formation from fluvial sandstones and coals of the Triunfo Member of the Rio Bonito Formation in the southeastern Paraná Basin (Fig. 1). In regions of the southern Paraná Basin, this sequence boundary locally separates crystalline basement and fluvial sandstones (SB-1 + 2 of Holz et al. [2006]). In the southeastern Paraná Basin, the fluvial sandstones of the Triunfo Member transition into the offshore mudstones of the

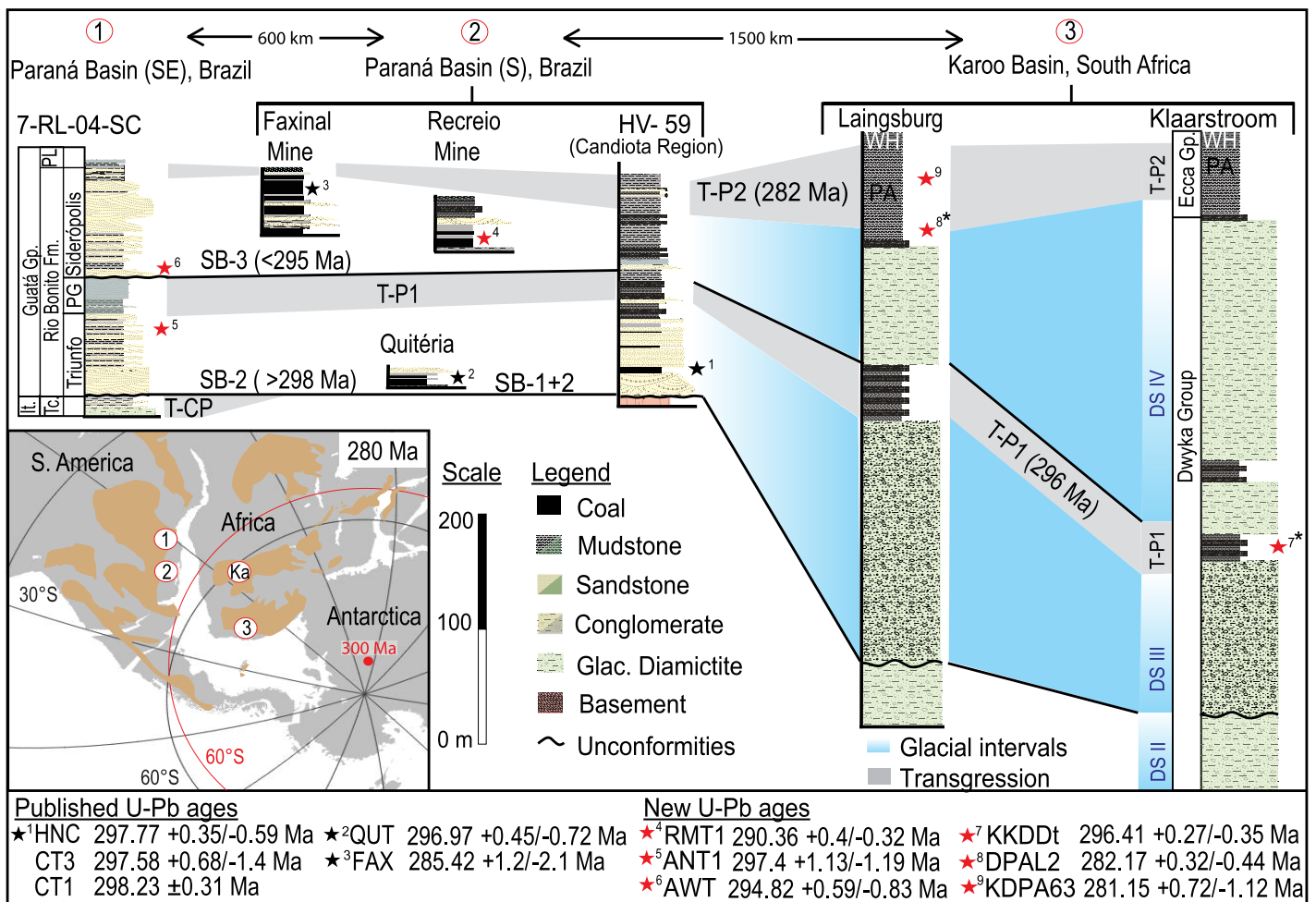


Figure 1. Stratigraphic columns of the core, outcrop, and mines for the southern and southeastern Paraná Basin, Brazil, and for the Karoo Basin, South Africa, calibrated by U-Pb zircon chemical abrasion thermal ionizing mass spectrometry (CA-TIMS) ages (see the Data Repository [see footnote 1]). Core HV-59 is located in the Candiota region of southern Brazil. The Karoo Basin section is modified after Visser (1997). DS II–DS IV are deglaciation sequences correlated across the Karoo Basin (Visser, 1997). Stars indicate stratigraphic position of CA-TIMS samples (black—published values [Griffis et al., 2018]; red—new data presented in this study). Asterisks (*) on age markers 7 and 8 denote sample locations reported by Bangert et al. (1999) and resampled and dated in this study. Gray bars are correlated marine transgressions: T-CP—transgression, Carboniferous-Permian; T-P1—transgression, Permian 1 (296 Ma); T-P2—transgression, Permian 2 (282 Ma). Approximate distances between regions are noted at top of figures. SB—sequence boundaries and interpreted ages (Holz et al., 2006); Gp.—Group; Fm.—Formation; It.—Itararé Group; Tc.—Taciba Formation; PG—Paraguaçu Member; PL—Palermo Formation; PA—Prince Albert Formation; WH—Whitehill Formation. Inset map: GPlates 2.1 (www.gplates.org) offset polar reconstruction of southwestern and south-central Gondwana at 280 Ma (Domeier and Torsvik, 2014). South Pole and 60°S latitude at 300 Ma are shown in red. Late Paleozoic depositional basins are shown in brown. 1—southeastern Paraná Basin; 2—southern Paraná Basin; 3—Karoo Basin; Ka—Kalahari Basin, southern Africa.

Paraguacú Member (T-P1 in Fig. 1). A second third-order sequence boundary (SB-3) separates offshore mudstones of the Paraguacú Member and fluvial to shallow marine sandstones of the Siderópolis Member (Fig. 1). In southern Brazil, SB-3 separates offshore mudstones from nearshore heterolithic mudstones, fluvial sandstones, and coals (Holz et al., 2006; Iannuzzi et al., 2010). The marine Palermo Formation overlies and interfingers laterally with the Rio Bonito Formation and is interpreted as the most widespread transgression of the early Permian succession (T-P2 in Fig. 1; see Holz et al., 2006). U-Pb zircon laser ablation inductively coupled plasma mass spectrometry (LA-ICP-MS) ages for volcanoclastic deposits sampled above SB-2 are variable and range from 298.8 ± 1.9 Ma to 281.3 ± 3.4 Ma, providing insufficient temporal resolution for constraining the unconformity (see the GSA Data Repository¹; Griffis et al., 2018).

The Karoo Basin of South Africa, located at $>60^{\circ}$ S during the latest Carboniferous and early Permian (Fig. 1; Domeier and Torsvik, 2014), hosts an up to 800-m-thick glaciogenic succession of that same age, which is divided into four deglaciation sequences (DS I–DS IV). These sequences are defined as clast-rich diamictite deposits overlain by clast-poor organic-rich mudstones and/or diamictite separated by unconformities, and are hypothesized to represent tectonic-eustatic cycles (Visser, 1997). The top of DS III is interpreted to represent the first major marine transgression into the Karoo Basin that can be traced across southern Africa and is dated by a U-Pb zircon secondary ion mass spectrometry (SIMS) age of 297 ± 1.8 Ma (age marker 7 in Fig. 1; Visser, 1997; Bangert et al., 1999; Stollhofen et al., 2008). DS III is overlain by a thick diamictite (100–300 m), which marks the return to glacial conditions in the Karoo Basin prior to terminal deglaciation (DS IV). The final deglaciation in the Karoo Basin is recorded by a thick marine mudstone in the basal Ecca Group (Prince Albert Formation) and culminates with a black shale (Whitehill Formation) (Fig. 1; Visser, 1997; Bangert et al., 1999) and is constrained to 289.6 ± 3.8 to 288.0 ± 3.0 Ma by SIMS U-Pb zircon ages for volcanoclastic deposits in the basal Ecca Group (age marker 8 in Fig. 1).

U-Pb ZIRCON CA-TIMS CHRONOSTRATIGRAPHY FOR SOUTHWESTERN TO SOUTH-CENTRAL GONDWANA

We present a chronostratigraphic framework for the Paraná and Karoo Basins, anchored by

new ($n = 6$) and recently published ($n = 5$; Griffis et al., 2018) U-Pb single-crystal zircon CA-TIMS ages for volcanoclastic deposits, in order to evaluate the synchronicity of the LPIA demise in South America and southern Africa, respectively (Fig. 1; see the Data Repository). A thorough description of samples, zircon treatments, and analytical techniques, including data tables and concordia and age-ranked plots, are presented in the Data Repository. The newly developed U-Pb zircon CA-TIMS–anchored chronostratigraphic framework indicates that a major deglaciation event occurred in both the Paraná (terminal deglaciation) and Karoo basins proximal to the Carboniferous-Permian boundary (CPB; T-CP in Fig. 1). Subsequent glaciation-deglaciation cycles in the Karoo Basin are synchronous with marine transgressions in the Paraná Basin in the early (ca. 296 Ma) and late early (282 Ma) Permian (T-P1 and T-P2 in Fig. 1).

Volcanoclastic deposits within the lowermost Rio Bonito Formation confirm a pre-CPB deglaciation age (298.9 Ma) for all glacial deposits in the southern to southeastern Paraná Basin (Cagliari et al., 2016; Griffis et al., 2018). U-Pb zircon CA-TIMS ages for volcanoclastics within the Candiota coals to the south (298.23 ± 0.31 Ma [sample CT1] to $297.77 + 0.35/-0.59$ Ma [sample HNC]; age marker 1 in Fig. 1), which can be traced into nearby core HV-59 (see the Data Repository for location), and for a volcanoclastic layer in the Triunfo Member in the southeastern Paraná Basin ($297.4 + 1.13/-1.19$ Ma [sample ANT1]; age marker 5 in Fig. 1) all constrain glaciation in these regions of the Paraná Basin to >298 Ma (Griffis et al., 2018). These volcanoclastics overlie a regional sequence boundary (SB-2 and SB 1 + 2; Fig. 1) by 30–60 m, indicating that inferred base-level fall was synchronous across the south to southeastern Paraná Basin. Glacial conditions in the Karoo Basin in the earliest Permian are recorded by thick (>100 m) diamictites (lower DS III; Fig. 1) and are hypothesized to be synchronous with the base-level fall in the Paraná Basin (SB-2). If confirmed, the terminal deglaciation in the southern Paraná Basin could be contemporaneous with the top of DS II in southern Africa dated at 302.0 ± 3.0 Ma to 299.2 ± 3.2 Ma (Visser, 1997; Bangert et al., 1999). High-resolution U-Pb zircon CA-TIMS ages for the upper Taciba Formation (Paraná Basin) and DS II (Kalahari Basin, southern Africa; Ka in Fig. 1) are now required to test this hypothesis (see the Data Repository).

In the Karoo Basin, subsequent glacial demise is indicated by thick (up to 200 m) glacial diamictites, which transition into glacially influenced transgressive mudstones and sandstones (top of DS III). A volcanic ash, located at the top of DS III, yields a U-Pb zircon CA-TIMS age of $296.41 + 0.27/-0.35$ Ma (age marker 7 in Fig. 1). Notably, this major transgression at the

top of DS III is traceable across southern Africa (Visser, 1997; Stollhofen et al., 2008) and contemporaneous with the transgressive Paraguacú Member (PG on Fig. 1) in the Paraná Basin. The age for Paraguacú Member is inferred based on the stratigraphic juxtaposition of marine mudstones over terrestrial and nearshore deposits, which are dated at $296.97 + 0.45/-0.72$ Ma (age marker 2 in Fig. 1; Griffis et al., 2018). The apparent synchronicity of the aforementioned transgressive surfaces, which record an abrupt shift to marine conditions throughout both depositional basins, is interpreted to record a substantial loss of continental ice at 296 Ma (plus or minus several hundred thousand years) (T-P1 in Fig. 1).

A final phase of glaciation in the Karoo Basin expressed by thick (200 m) diamictites (lower DS IV), which overlie transgressive mudstones (top of DS III), occurred in the early Permian (Visser, 1997). In the Paraná Basin, an erosional unconformity (SB-3 in Fig. 1) separates marine deposits of the Paraguacú Member from fluvial deposits of the overlying Siderópolis Member. The SB-3 unconformity has been interpreted as representing a forced regression, driven by major base-level fall (Holz et al., 2006). A U-Pb zircon CA-TIMS age for a volcanoclastic layer sampled between two fluvial sandstones (Alfredo Wagner locality), which overlie marginal marine mudstones that can be traced into nearby core 7-RL-04-SC, provides a minimum age for the onset of SB-3 of $294.82 + 0.59/-0.83$ Ma (age marker 6 in Fig. 1). In the southern Paraná Basin, volcanoclastic layers sampled from terrestrial coal deposits above SB-3 from the Recreio (age marker 4 in Fig. 1) and Faxinal (age marker 3 in Fig. 1) mines yield ages of $290.36 + 0.4/-0.32$ Ma and $285.42 + 1.2/-2.1$ Ma, respectively, indicating that low base level persisted in this region of the Paraná Basin into the Permian. (For location information, see the Data Repository.)

Terminal deglaciation (DS IV) in the Karoo Basin is recorded by a thick (100 m) interval of turbidite deposits of the Prince Albert Formation that is capped by black shales of the Whitehill Formation (T-P2 in Fig. 1; Visser, 1997). Volcanic ash layers sampled from the lower (age marker 8 in Fig. 1) and middle (age marker 9 in Fig. 1) Prince Albert Formation yield new U-Pb zircon CA-TIMS ages of 282.17 Ma $+ 0.32/-0.44$ and $281.15 + 0.72/-1.12$ Ma, respectively, indicating that this region of south-central Gondwana was fully deglaciated by 282 Ma. In the Paraná Basin, marine mudstones and sandstones of the Palermo Formation (PL in Fig. 1) overlie fluvial and shallow marine sandstones of the Siderópolis Member (southeastern Paraná Basin) and the Faxinal and Recreio mine coals (southern Paraná Basin). The Palermo marine deposits are interpreted as recording a major transgression, consistent with ice loss in southwestern and south-central Gondwana (T-P2 in Fig. 1; Holz et al., 2010).

¹GSA Data Repository item 2019387, sample location and descriptions, laboratory and analytical techniques, data tables, concordia diagrams, and age ranked plots, is available online at <http://www.geosociety.org/datarepository/2019/>, or on request from editing@geosociety.org.

CO₂ -FORCED DEGLACIATION

Reconstructed atmospheric $p\text{CO}_2$ for the latest Pennsylvanian and early Permian indicates a stepped rise from a minimum across the CPB to maximum concentrations ($<2\times$ present atmospheric level [PAL]) toward the end of the early Permian, which is consistent with the presented stepwise deglaciation history (Fig. 2; Montañez et al., 2007; revised in Richey et al., 2017). Terminal deglaciation in the Paraná Basin, which occurred proximal to but before the CPB, coincides with overall high $p\text{CO}_2$ ($>1\times$ PAL) through the latest Carboniferous (Fig. 2). Return to glacial conditions in the Karoo Basin in the earliest Permian (DS III), which coincides with regional base-level fall (SB-2) in the Paraná Basin, is synchronous with a drop in $p\text{CO}_2$ ($0.5\times$ PAL). The demise of DS III in the Karoo Basin, synchronous with the Paraguaçu transgression, is coincident with a renewed rise in $p\text{CO}_2$ to PAL (296 Ma). A return of ice in the Karoo Basin, coincident with a base-level fall (SB-3) in the Paraná Basin, is synchronous with a second CO₂ fall to $0.5\times$ PAL at 295 Ma. Terminal demise of glaciation in the Karoo Basin occurred during a protracted CO₂ rise through the remainder of the early Permian (Fig. 2). Overlap in timing of inferred deglaciations and base-level rises with stepwise increases in $p\text{CO}_2$ suggests that stepwise and near-synchronous deglaciation across southwestern and south-central Gondwana was likely greenhouse-gas forced. Notably, the repeated return to glacial conditions in the

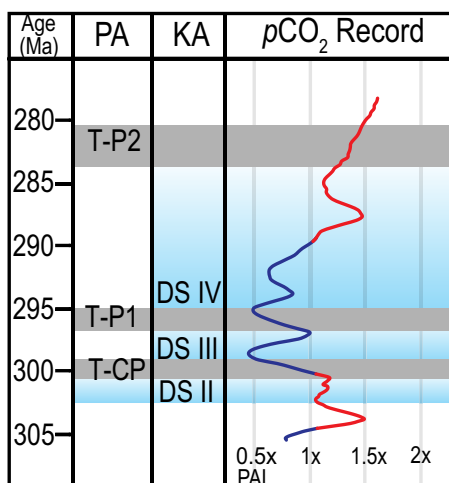


Figure 2. Low-latitude paleosol-carbonate-based $p\text{CO}_2$ record (Montañez et al., 2007; modified by Richey et al., 2017), shown as variation relative to present atmospheric level (PAL; 400 ppm). Blue—lower than PAL; red—higher than PAL; T-CP—transgression, Carboniferous-Permian; T-P1—transgression, Permian 1 (296 Ma); T-P2—transgression, Permian 2 (282 Ma). DS II–DS IV are deglaciation sequences correlated across the Karoo Basin (Visser, 1997). CO₂ tracks with the glaciation history in the Paraná (PA; Brazil) and Karoo (KA; South Africa) Basins during the early Permian.

higher-latitude ($>60^\circ\text{S}$) Karoo Basin, while the lower-latitude Paraná Basin ($<55^\circ\text{S}$) remained ice free, indicates the superimposed influence of additional regional drivers (e.g., paleogeography, topography, and atmospheric moisture) on local to regional thresholds for ice accumulation in southern Gondwana (Isbell et al., 2012; Montañez and Poulsen, 2013).

ACKNOWLEDGMENTS

We thank Companhia de Pesquisa de Recursos Minerais (CPRM) for access to core in Caçapava do Sul in Rio Grande do Sul State (Brazil). We thank Nelson Mandela University and Maarten De Wit for field assistance in South Africa. This manuscript greatly benefited from constructive review by Fernando Corfu, Urs Schaltegger, and two anonymous referees. This study was funded by U.S. National Science Foundation awards OIES-1444210 to Montañez and Isbell, EAR-1729882 to Montañez and Yin, EAR-1728705 to Mundil, and EAR-1729219 to Isbell. Additional support was provided by the Brazilian Research Council (PQ 309211/2013-1) and the Foundation for Research Support of Rio Grande do Sul State (FAPERGS; process PqG 10/1584-6) to Iannuzzi. Sample analysis at the Berkeley Geochronology Center was supported by the Ann and Gordon Getty Foundation.

REFERENCES CITED

- Bangert, B., Stollhofen, H., Lorenz, V., and Armstrong, R., 1999, The geochronology and significance of ash-fall tuffs in the glaciogenic Carboniferous-Permian Dwyka Group of Namibia and South Africa: *Journal of African Earth Sciences*, v. 29, p. 33–49, [https://doi.org/10.1016/S0899-5362\(99\)00078-0](https://doi.org/10.1016/S0899-5362(99)00078-0).
- Cagliari, J., Philipp, R.P., Buso, V.V., Netto, R.G., Hillebrand, P.K., da Cunha Lopes, R., Basei, M.A.S., and Faccini, U.F., 2016, Age constraints of the glaciation in the Paraná Basin: Evidence from new U-Pb dates: *Journal of the Geological Society*, v. 173, p. 2015–2161, <https://doi.org/10.1144/jgs2015-161>.
- Crowell, J.C., 1983, Ice ages recorded on Gondwanan continents: *South African Journal of Geology*, v. 86, p. 237–262.
- Domeier, M., and Torsvik, T.H., 2014, Plate tectonics in the late Paleozoic: *Geoscience Frontiers*, v. 5, p. 303–350, <https://doi.org/10.1016/j.gsf.2014.01.002>.
- Franco, D.R., Ernesto, M., Ponte-Neto, C.F., Hinnov, L.A., Berquó, T.S., Fabris, J.D., and Rosière, C.A., 2012, Magnetostratigraphy and mid-paleolatitude VGP dispersion during the Permo-Carboniferous Superchron: Results from Paraná Basin (Southern Brazil) rhythmites: *Geophysical Journal International*, v. 191, p. 993–1014, <https://doi.org/10.1111/j.1365-246X.2012.05670.x>.
- Gastaldo, R.A., DiMichele, W.A., and Pfefferkorn, H.W., 1996, Out of the icehouse into the greenhouse: A late Paleozoic analog for modern global vegetational change: *GSA Today*, v. 6, no. 10, p. 1–7.
- Griffis, N.P., Mundil, R., Montañez, I.P., Isbell, J., Fedorchuk, N., Vesely, F., Iannuzzi, R., and Yin, Q.-Z., 2018, A new stratigraphic framework built on U-Pb single zircon TIMS ages with implications for the timing of the penultimate icehouse (Paraná Basin, Brazil): *Geological Society of America Bulletin*, v. 130, p. 848–858, <https://doi.org/10.1130/B31775.1>.
- Holz, M., Kühle, J., Philipp, R.P., Bischoff, A.P., and Arima, N., 2006, Hierarchy of tectonic control on stratigraphic signatures: Base-level changes during the Early Permian in the Paraná Basin, southernmost Brazil: *Journal of South American Earth Sciences*, v. 22, p. 185–204, <https://doi.org/10.1016/j.jsames.2006.09.007>.
- Holz, M., França, A.B., Souza, P.A., Iannuzzi, R., and Rohn, R., 2010, A stratigraphic chart of the Late Carboniferous/Permian succession of the eastern border of the Parana Basin, Brazil, South America: *Journal of South American Earth Sciences*, v. 29, p. 381–399, <https://doi.org/10.1016/j.jsames.2009.04.004>.
- Iannuzzi, R., Souza, P.A., and Holz, M., 2010, Stratigraphic and paleofloristic record of the Lower Permian postglacial succession in the southern Brazilian Paraná Basin, in López-Gamundi, O.R., and Buatois, L.A., eds., *Late Paleozoic Glacial Events and Postglacial Transgressions in Gondwana: Geological Society of America Special Paper 468*, p. 113–132, [https://doi.org/10.1130/2010.2468\(05\)](https://doi.org/10.1130/2010.2468(05)).
- Isbell, J.L., Henry, L.C., Gulbranson, E.L., Limarino, C.O., Fraiser, M.L., Koch, Z.J., Ciccioli, P.L., and Dineen, A.A., 2012, Glacial paradoxes during the late Paleozoic ice age: Evaluating the equilibrium line altitude as a control on glaciation: *Gondwana Research*, v. 22, p. 1–19, <https://doi.org/10.1016/j.gr.2011.11.005>.
- Limarino, C.O., Césari, S.N., Spalletti, L.A., Taboada, A.C., Isbell, J.L., Geuna, S., and Gulbranson, E.L., 2014, A paleoclimatic review of southern South America during the late Paleozoic: A record from icehouse to extreme greenhouse conditions: *Gondwana Research*, v. 25, p. 1396–1421, <https://doi.org/10.1016/j.gr.2012.12.022>.
- Lowry, D.P., Poulsen, C.J., Horton, D.E., Torsvik, T.H., and Pollard, D., 2014, Thresholds for Paleozoic ice sheet initiation: *Geology*, v. 42, p. 627–630, <https://doi.org/10.1130/G35615.1>.
- McKenzie, N.R., Horton, B.K., Loomis, S.E., Stockli, D.F., Planavsky, N.J., and Lee, C.-T.A., 2016, Continental arc volcanism as the principal driver of icehouse-greenhouse variability: *Science*, v. 352, p. 444–447, <https://doi.org/10.1126/science.aad5787>.
- Miller, K.G., Kominz, M.A., Browning, J.V., Wright, J.D., Mountain, G.S., Katz, M.E., Sugarman, P.J., Cramer, B.S., Christie-Blick, N., and Pekar, S.F., 2005, The Phanerozoic record of global sea-level change: *Science*, v. 310, p. 1293–1298, <https://doi.org/10.1126/science.1116412>.
- Montañez, I.P., and Poulsen, C.J., 2013, The late Paleozoic ice age: An evolving paradigm: *Annual Review of Earth and Planetary Sciences*, v. 41, p. 629–656, <https://doi.org/10.1146/annurev.earth.031208.100118>.
- Montañez, I.P., Tabor, N.J., Niemeier, D., DiMichele, W.A., Frank, T.D., Fielding, C.R., Isbell, J.L., Birgenheuer, L.P., and Rygel, M.C., 2007, CO₂-forced climate and vegetation instability during late Paleozoic deglaciation: *Science*, v. 315, p. 87–91, <https://doi.org/10.1126/science.1134207>.
- Montañez, I.P., McElwain, J.C., Poulsen, C.J., White, J.D., DiMichele, W.A., Wilson, J.P., Griggs, G., and Hren, M.T., 2016, Climate, $p\text{CO}_2$ and terrestrial carbon cycle linkages during late Paleozoic glacial-interglacial cycles: *Nature Geoscience*, v. 9, p. 824–828, <https://doi.org/10.1038/ngeo2822>.
- Richey, J., Montañez, I., Looy, C., DiMichele, W., and White, J., 2017, Revisiting early Permian CO₂ via improved input parameters and models: *Geological Society of America Abstracts with Programs*, v. 49, no. 6, <https://doi.org/10.1130/abs/2017AM-300828>.
- Rocha-Campos, A.C., dos Santos, P.R., and Canuto, J.R., 2008, Late Paleozoic glacial deposits of Brazil: Parana Basin, in Fielding, C.R., et al.,

- eds., Resolving the Late Paleozoic Ice Age in Time and Space: Geological Society of America Special Paper 441, p. 97–114, [https://doi.org/10.1130/2008.2441\(07\)](https://doi.org/10.1130/2008.2441(07)).
- Schneider, R.L., Mühlmann, H., Tommasi, E., Medeiros, R.A., Daemon, R.F., and Nogueira, A.A., 1974, Revisão estratiográfica da Bacia do Paraná, in Proceedings, Congresso Brasileiro de Geologia XXVIII, Porto Alegre: Porto Alegre, Sociedade Brasileira de Geologia, v. 1, p. 41–66.
- Stollhofen, H., Werner, M., Stanistreet, I.G., and Armstrong, R.A., 2008, Single-zircon U-Pb dating of Carboniferous-Permian tuffs, Namibia, and the intercontinental deglaciation cycle framework, in Fielding, C.R., et al., eds., Resolving the Late Paleozoic Ice Age in Time and Space: Geological Society of America Special Paper 441, p. 83–96, [https://doi.org/10.1130/2008.2441\(06\)](https://doi.org/10.1130/2008.2441(06)).
- Vesely, F.F., and Assine, M.L., 2004, Sequências e tratos de sistemas deposicionais do Grupo Itararé, norte do Estado do Paraná: Revista Brasileira de Geociências, v. 34, p. 219–230, <https://doi.org/10.25249/0375-7536.2004342219230>.
- Visser, J.N.J., 1997, Deglaciation sequences in the Permian-Carboniferous Karoo and Kalahari basins of southern Africa: A tool in the analysis of cyclic glaciomarine basin fills: Sedimentology, v. 44, p. 507–521, <https://doi.org/10.1046/j.1365-3091.1997.d01-35.x>.

Printed in USA